# Synthesis of narrow band gap SnTe nanocrystals: Nanoparticles and single crystal nanowires via oriented attachment

**ARTICLE** *in* CRYSTENGCOMM · DECEMBER 2010

Impact Factor: 4.03 · DOI: 10.1039/c004098n



**8 AUTHORS**, INCLUDING:

Jiajia Ning
Hebrew University of Jerusalem
**19** PUBLICATIONS **411** CITATIONS
SEE PROFILE

Bo Zou
Harbin Institute of Technology
**187** PUBLICATIONS **2,405** CITATIONS
SEE PROFILE

# Synthesis of narrow band gap SnTe nanocrystals: nanoparticles and single crystal nanowires *via* oriented attachment†

**Jiajia Ning,[ab] Kangkang Men,[a] Guanjun Xiao,[a] Bo Zou,*[a] Li Wang,[b] Quanqin Dai,[a] Bingbing Liu[a] and Guantian Zou[a]**

***Received 9th March 2010, Accepted 10th June 2010***
**DOI: 10.1039/c004098n**

SnTe nanocrystals with different shapes and sizes are synthesized by a simple and facile method. The length of the fatty chain in amine has an important effect on the shape and size of SnTe nanocrystals. When oleylamine (OLA) is used as ligand, SnTe nanoparticles with size of 4 nm and high crystallinity are produced. However, when octylamine (OTA) is used as ligand, larger SnTe nanoparticles with low crystallinity are achieved, which would transform into single crystal SnTe nanowires with increasing reaction time. The driving force of shape evolution of SnTe nanocrystals is reducing the high surface free energy. An oriented attachment mechanism is proposed to explain the transition from nanoparticles to nanowires, and oriented attachment of nanoparticles to single crystal nanowires is proposed to reduce the interface energy by the greatest amount.

## Introduction

Semiconductor nanocrystals with narrow band-gap is a focus in scientific research and fundamental applications in the last decades. It can be widely used in optical, electronic, optoelectronic, infrared (IR) and near infrared (NIR) detectors, IR and NIR emission, and solar cells.[1] A number of series of narrow band-gap semiconductor nanocrystals (NSNCs) have been synthesized, such as II–VI (HgTe, $Cd_xHg_{1-x}Te$),[2] III–V (InP, InAs and GaAs),[3] IV–VI (PbS and PbSe)[4] and I–III–VI ($CuInS_2$ and $CuInSe_2$).[5] However, the emission spectra of these reported NSNCs are smaller than 3 μm—few emission spectra of NSNCs can cover the middle infrared (MIR) region (3–6 μm). The MIR emission spectra have potential for low band-gap detectors, long wavelength-range laser diodes, thermal imaging, chemical process control, environmental monitoring of atmospheric pollution, and free space optical communications.[6] Till now, the IV–VI lead salt and III–V Sb compound are the main choices for MIR emission. However, the low thermal conductivity, high continuous wave output power and toxicity of lead salt prevent its use in many fields.[7] The III–V Sb compounds are mainly GaSb, InSb, InPSb, InAsSb, GaInAsSb,[8] *etc.*, which are produced by MOCVD. The complex synthesis process, expensive and toxic raw materials are disadvantages to their applications. Moreover, the emission spectra of III–V Sb compounds (3–5 μm) have limitations in the MIR region. Scientists have paid attention to synthesis of new structures to get MIR emission spectra. The quantum well and super lattice have been identified for MIR spectra.[9] However, the production process of quantum well and super lattice is very complex and the cost is very high. Synthesis of new, simple and cheap semiconductors (or structures) by facile synthetic route is a challenge in synthetic chemistry and materials science.

SnTe is an IV–VI semiconductor with direct band gap of 0.18 eV in bulk material at room temperature, and is an important material for MIR photodetectors and thermoelectric heat converters.[10] Bulk SnTe has the cubic rock-salt crystal structure (space group *Fm*3*m*),[10] which is different from other layered crystal structures, IV–VI tin chalcogenides (SnS, SnSe). SnTe is an important narrow band gap semiconductor. However, compared to other semiconductor nanocrystals, the reports on SnTe nanocrystals are few.[11] Based on the quantum-size effect, the emission spectra in SnTe nanocrystals can cover the MIR region (3–6 μm) and far infrared region (> 6μm). Talapin and his co-workers have synthesized SnTe nanoparticles with obvious quantum-size effect, and the absorbance spectra of 7.2 nm SnTe nanoparticles reaching 2.5 μm.[11d] However, the toxic, expensive, air and water sensitive organic metallic $Sn[N(SiMe_3)_2]_2$ is used as tin precursor, which increases the experimental cost and experimental process. Much more effort needs to be paid for improving the synthetic routes and research on properties of SnTe nanocrystals.

Herein, we synthesize SnTe nanoparticles with different sizes by using ligands with different lengths of alkyl chains *via* a simple and facile method. Single crystal SnTe nanowires would be formed by oriented attachment of nanoparticles. A simple tin oxide hydroxide ($Sn_6O_4(OH)_4$) is introduced as tin precursor for the synthesis of SnTe nanocrystals; $Sn_6O_4(OH)_4$ can be synthesized easily.[12] Telluronium, which is dissolved in tri-n-octylphosphine (TOP), is used as Te precursor. When the oleylamine (OLA) is used as ligand, SnTe nanoparticles with small size and high crystallinity are produced. However, when octylamine (OTA) is used as ligand, SnTe nanoparticles with poor crystallinity are produced first, and then these SnTe nanoparticles grow to single crystal SnTe nanowires by oriented attachment. The

[a]*State Key Laboratory of Superhard Materials, Jilin University, Changchun, 130012, P. R. China. E-mail: zoubo@jlu.edu.cn; Fax: +86-431-85168883; Tel: +86-431-85168882*
[b]*Department of Material Science and Engineering, Jilin Univeristy, Changchun, 130012, P. R. China*

† Electronic supplementary information (ESI) available: Selected area electron diffraction (SAED) of SnTe nanocrystals and high resolution transmission electron microscopy (HRTEM) images for other single crystal SnTe nanowires. See DOI: 10.1039/c004098n

driving force of attachment of nanoparticles to single nanowires is the reduction of the high free energy of nanocrystals. The effects of ligands to the size and shape of SnTe nanocrystals have been discussed.

## Experimental

### Chemical reagent

$SnCl_2$ (98%), tri-n-octylphosphine (TOP, 90%), 1-octadecene (ODE, 90%), oleic acid (OA, 90%) and tellurium (Te, 99.99%) were purchased from Aldrich. Oleylamine (OLA, ≥70%) and octylamine (OTA, 98%) were purchased from Fluka. Toluene, chloroform, and methanol were purchased from the Beijing Chemical Company. All chemicals were used in the experiments without further purification.

### Synthesis section

All experiments were carried out using standard airless techniques: a vacuum/dry nitrogen gas Schlenk line was used for synthesis and a nitrogen glove-box for storing and handling air- and moisture-sensitive chemicals. The TOP-Te solution (0.25mmol $ml^{-1}$) was prepared by dissolving elemental tellurium in TOP at 250 °C for 2 h with nitrogen gas protection.

(1) Synthesis of $Sn_6O_4(OH)_4$:[12] $SnCl_2$ (0.1517 g, 0.800 mmol), OLA (1.9224 g, 7.200 mmol), and ODE (0.9072 g, 3.600 mmol) were loaded into a three-neck flask in a glove-box. Then, the sealed flask was taken out and connected to the Schlenk line with nitrogen flow. After 20 μL of $H_2O$ was injected into the flask, a yellow precipitate could be observed at room temperature. The stirring was continued for a few minutes. The yellow precipitate was collected by centrifuging. The sample was purified by toluene and then dried at 50 °C.

(2) Synthesis of SnSe nanocrystals: $Sn_6O_4(OH)_4$ (0.0422 g, 0.05 mmol), OA (1 mL) and OLA (or OTA) (10 ml) were placed into a 50 ml three-neck flask in a glove-box. Then the flask was taken out and connected to a Schlenk line. The flask was evacuated and flushed a few times with nitrogen to remove oxygen and subsequently heated to 180 °C. This solution was kept at 180 °C for 30 min to dissolve $Sn_6O_4(OH)_4$ and remove water. Then 1.2 mL of TOP-Te (0.25 mmol $mL^{-1}$) was added with a syringe. The solution became dark red as soon as the TOP-Te solution was injected and the temperature lowered to 165 °C. At different reaction moments, aliquots were taken from the reaction flask and immediately quenched to room temperature in toluene. An equal volume of methanol was added into the solution and nanocrystals were collected by centrifuging. These nanocrystals were purified three times. Finally, the nanocrystals were dissolved in nonpolar solvents, forming stable concentrated colloidal solutions.

### Characterization

Powder X-ray diffraction (XRD) was performed on a Bruker D8 diffractometer operating at 40 kV and 40 mA, using Cu Kα radiation. Data were collected from 15° to 80° with a sampling interval 0.02° per step and a counting rate of 0.2 s per step. Transmission electron microscopy (TEM) images and selected area electron diffraction (SAED) were obtained in a Hitachi H-8100IV transmission electron microscope using an acceleration voltage of 200 kV. High resolution transmission electron microscopy (HRTEM) images were taken with a JEOL JEM-2100 at 200kV. The point-to-point resolution of this HRTEM is 0.19 nm.

## Results and discussion

The crystal structure and chemical composition of the as-prepared samples are characterized by powder X-ray diffraction (XRD), as shown in Fig. 1. All diffraction peaks correspond to the cubic rock-salt crystal structure of SnTe (space group: *Fm*3*m* and JCPDS no. 65-0322). The lattice parameters are $a = 6.304$ Å, $\alpha = \beta = \gamma = 90$ °C. The obvious diffraction peaks could be indexed to the (200), (220), (311), (222), (420) and (422) planes of the rock-salt crystal structure of SnTe. No other diffraction peaks can be observed in Fig. 1, indicating no other crystal structure and chemical composition compounds are in existence in the sample. The weak and wide diffraction peaks are due to the smaller size of SnTe nanocrystals. Selected area electron diffraction (SAED) of SnTe nanocrystals is given in Fig. S1.† The diffraction rings in SAED correspond to the (200), (220), (222) and (400) planes of the cubic rock-salt crystal structure of SnTe. The crystal structure of SnTe nanocrystals from SAED agrees with that from XRD.

The shape and size of the produced SnTe nanocrystals are characterized by transmission electron microscopy (TEM) and high resolution transmission electron microscopy (HRTEM). Fig. 2 gives the TEM and HRTEM images of the SnTe nanocrystals produced with OLA and OTA. The SnTe nanoparticles are about 4 nm in size and the size distribution is uniform. The crystallinity of SnTe nanoparticles is good, the lattice of SnTe nanoparticles can be observed in HRTEM images (Fig. 2b). The shape and size of SnTe nanocrystals synthesized when OTA was used as ligand and solution are also given in Fig. 2. At the beginning of the reaction, the products are nanoparticles with sizes of about 8 nm. The SnTe nanoparticles have low crystallinity—no regular lattice can be observed in nanoparticles (insert in Fig. 2c). Then, the low crystallinity SnTe nanoparticles would transform into SnTe nanowires when prolonging the reaction time, as shown in Fig. 2d. The SnTe nanowires are about 50 nm in length and 5 nm in width. These results show that ligands have

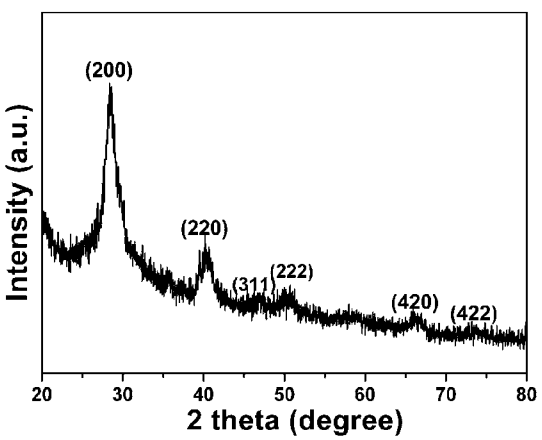


**Fig. 1** XRD patterns of as-prepared SnTe nanocrystals.

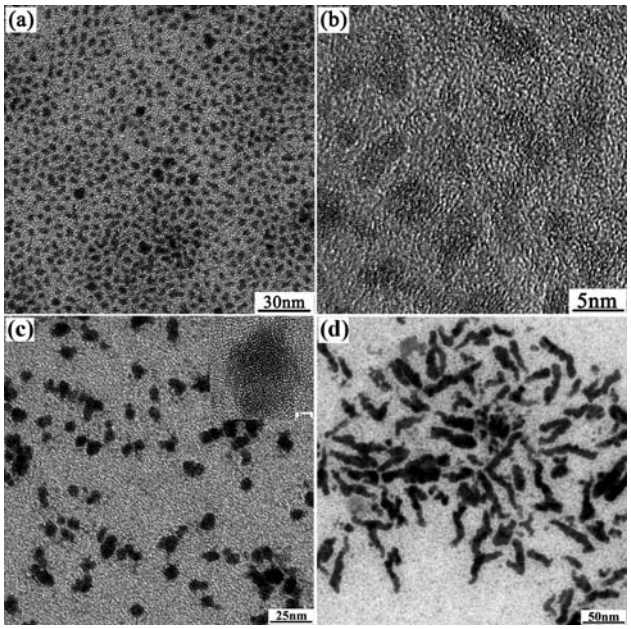


**Fig. 2** TEM images of SnTe nanoparticles (a) and HRTEM images of SnTe nanoparticles (b), which are synthesized by OLA as solution and ligands. TEM images of SnTe nanoparticles (c) and SnTe nanowires (d), which are synthesized by OTA as solution and ligands.

important effects on the shape and size of products. The difference between OLA and OTA is the length of the fatty chain; these effects on SnTe nanocrystals are mainly induced by the length of the fatty chain in amine ligands. When the reaction is below the boiling point of the amines, the shorter length of fatty chain would induce a faster growth rate of nanocrystals. The faster growth rate of nanocrystals would cause a larger size and lower crystallinity of nanocrystals.[13] In our experiment, we get SnTe nanocrystals with size of 4 nm with OLA as ligands, and nanoparticles with 8 nm and low crystallinity would be produced with OTA as ligands. The reaction temperature (165 °C) is lower than the boiling point of OLA (348 °C) and OTA (175 °C). The shorter length of fatty chain OTA would induce a larger size of SnTe nanoparticles, and the low crystallinity is induced by the greater dynamics on the surface of nanocrystals.

SnTe nanowires are investigated by HRTEM for getting the detailed structure and formation mechanism of the nanowires, as shown in Fig. 3. SnTe nanowires have good crystallinity, and the lattice can be seen clearly. Fig. 3a, b, c and d give the detailed crystal structure of different parts in these SnTe nanowires, respectively. The plane distance of 0.315 nm corresponds to the (200) lattice fringe of the cubic rock-salt crystal structure of SnTe, which has been observed in every area of SnTe nanowires. SnTe nanowires grow along the <100> direction. Some defects are in existence in the nanowires, but no attachment on the surface or boundaries can be observed in SnTe nanowires. All of these results show SnTe nanowires are single crystalline in structure. Other SnTe nanowires with the single crystal structure are also characterized by HRTEM (Fig. S2†). Fig. 3e gives the crystal structure model of SnTe nanowires, which grow by (200) planes along the <100> direction. In the experiment, SnTe nanowires would grow to bigger nanowires when increasing the reaction time (Fig. 4). The bigger SnTe nanowire is 150 nm in length and 10 nm in width. HRTEM images show this bigger SnTe nanowire to be single crystalline, and only some defects are observed in this single crystal nanowire. The single crystalline structure of SnTe nanowires has not been changed in the growth process. Fig. 5 gives the TEM images of the attachment of SnTe nanoparticles to single crystal nanowires. The products are individual SnTe nanoparticles at the initial stage of the reaction (2 min). Fig. 5b shows the attachment stage of nanoparticles (both smaller nanowires and single nanoparticles can be observed). When increasing the reaction time to 7 min, the nanoparticles would attach to single crystal nanowires (Fig. 5c). The single crystal SnTe nanowires would grow bigger with increasing reaction time (Fig. 5d).

One-dimensional (1-D) nanocrystal materials, including nanorods and nanowires, have been intensively investigated because of their unique properties, which are derived from their low dimensionality.[14] It is very interesting that zero-dimensional (0-D) nanoparticles can aggregate to single crystal 1-D

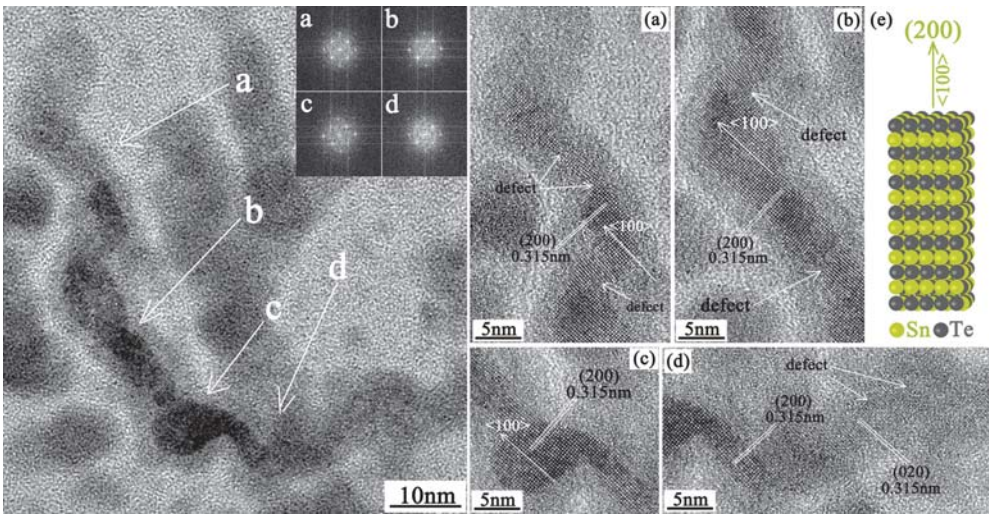


**Fig. 3** HRTEM images, SAED images and crystal model of single crystalline SnTe nanowires.

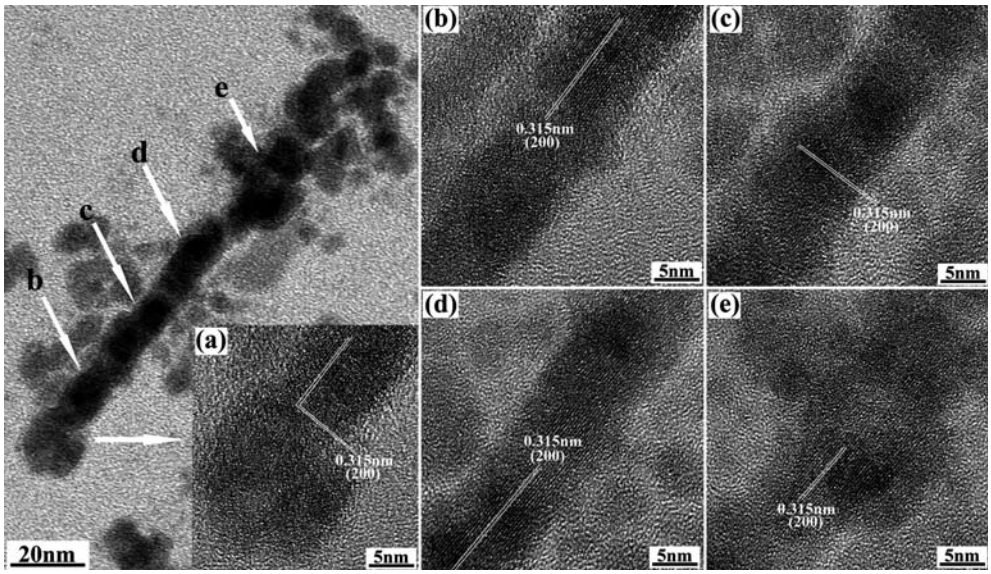


**Fig. 4** HRTEM images of longer single crystal SnTe nanowires.

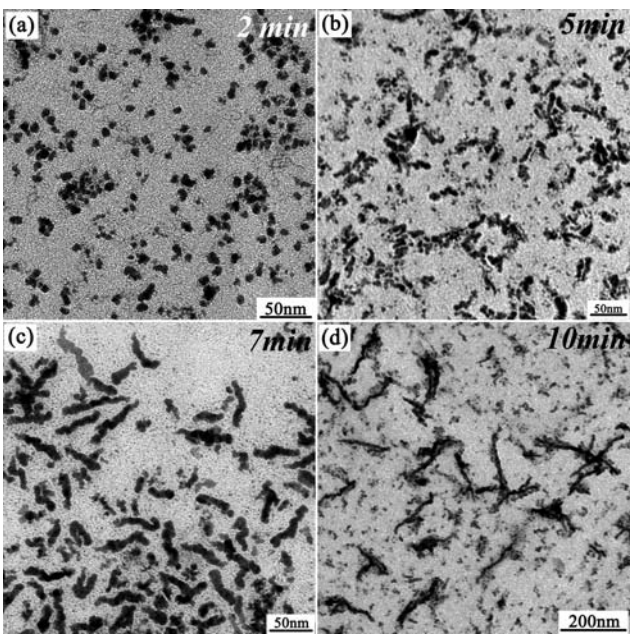


**Fig. 5** TEM images of attachment of SnTe nanoparticles to nanowires. When increasing the reaction time, the SnTe nanoparticles transformed to single crystal SnTe nanowires. SnTe nanoparticles (a), mixture of nanoparticles and short nanowires (b), nanowires (c) and longer nanowires (d).

nanowires by oriented attachment, which has been observed in a few nanocrystals.[15] Herein, we synthesize novel single crystalline SnTe nanowires by aggregation of SnTe nanoparticles. Because the shorter length of fatty chain in amines induces more dynamics on the surface of nanocrystals,[13] SnTe nanoparticles have higher surface free energy which is derived from defects and low crystallinity. These low crystallinity SnTe nanoparticles would tend to a lower energy state. The oriented attachment mechanism is proposed to explain the shape evolution of SnTe

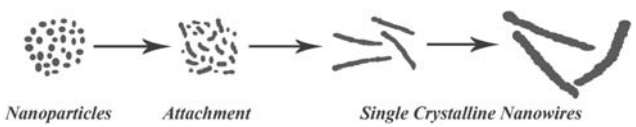


**Fig. 6** The schematic illustration of the evolution from SnTe nanoparticles to single crystal SnTe nanowires.

nanocrystals (Fig. 6). SnTe nanoparticles with the rock salt structure have three equivalent <100> directions, which tend to grow bigger nanoparticles to reduce free energy. However, comparing attachment of SnTe nanoparticles to nanowires, growth smaller nanoparticles to bigger ones is not a more effective way to reduce high surface free energy. The oriented attachment process can be more effective at reducing surface area than growth to bigger nanoparticles. In our experiment, SnTe nanoparticles attaching themselves to nanowires is a preferred way to reduce high surface free energy. Among various types of attachments, attachment of 0-D nanoparticles to a single nanocrystal can reduce the interface energy by the greatest amount.[15d] SnTe nanoparticles transform to single crystal nanowires by oriented attachment; attachment of surfaces or boundaries could not be observed in nanowires. The continuous growth of nanowires can further reduce the free energy by reducing the surface area of nanocrystals. Coupled with the attachment process, the crystallinity of nanocrystals has been improved distinctly (Fig. 3 and 4).

## Conclusions

In conclusion, narrow band gap SnTe nanocrystals with different shapes and sizes have been synthesized by using different ligands. Single crystal SnTe nanowires are produced by oriented attachment of nanoparticles. When ligands have longer fatty chains, the produced SnTe nanoparticles have smaller sizes and high crystallinity. However, larger size and low crystallinity SnTe nanoparticles would be produced with short length ligands. The

 

low crystallinity SnTe nanoparticles would then transform into single crystal SnTe nanowires. The effects of ligands to the shape and size of produced SnTe nanocrystals have been discussed. An oriented attachment mechanism is proposed to explain the aggregation of nanoparticles to nanowires. The driving force of attachment of nanoparticles to nanowires is the reduction of the high free energy of nanocrystals. Attachment of nanoparticles to single crystal nanowires can decrease the largest free energy. Coupled with the attachment process, the crystallinity of nanocrystals has been improved, which can also decrease the free energy of nanocrystals. This work would improve the studies on IV–VI SnTe nanocrystals, and provide a new case for oriented attachment.

## Acknowledgements

This work was supported by NSFC (Nos. 20773043, and 10979001), the National Basic Research Program of China (No. 2005CB724400 and No. 2007CB808000).

## Notes and references

1 (*a*) R. D. Schaller, M. A. Pertruska and V. I. Klimov, *J. Phys. Chem. B*, 2003, **107**, 13765–13768; (*b*) D. V. Talapin and C. B. Murray, *Science*, 2005, **310**, 86–89; (*c*) M. S. Dresselhaus, G. Chen, M. Y. Tang, R. Yang, H. Lee, D. Wang, Z. Ren, J. P. Fleurial and P. Gogna, *Adv. Mater.*, 2007, **19**, 1043–1053; (*d*) H. Qian, C. Dong, J. Peng, X. Qiu, Y. Yu and J. Ren, *J. Phys. Chem. C*, 2007, **111**, 16852–16857; (*e*) M. Böberl, M. V. Kovalenko, S. Gamerith, E. List and W. Heiss, *Adv. Mater.*, 2007, **19**, 3574–3578.

2 (*a*) A. Rogach, S. Kershaw, M. Burt, M. Harrison, A. Kornowski, A. Eychmüller and H. Weller, *Adv. Mater.*, 1999, **11**, 552–555; (*b*) S. V. Kershaw, M. Burt, M. Harrison, A. L. Rogach, H. Weller and A. Eychmüller, *Appl. Phys. Lett.*, 1999, **75**, 1694–1696; (*c*) V. Lesnyak, A. Lutich, N. Gaponik, M. Grabolle, A. Plotnikov, U. Resch-Genger and A. Eychmüller, *J. Mater. Chem.*, 2009, **19**, 9147–9152; (*d*) Z. Yang, Z. H. Sun, T. Ming, G. S. Li, J. F. Wang and J. C. Yu, *J. Mater. Chem.*, 2009, **19**, 7002–7010.

3 (*a*) J. C. Hsieh, D. S. Yun, E. Hu and A. M. Belcher, *J. Mater. Chem.*, 2010, **20**, 1435–1437; (*b*) R. G. Xie, D. Battaglia and X. G. Peng, *J. Am. Chem. Soc.*, 2007, **129**, 15432–15433; (*c*) Z. P. Liu, A. Kumbhar, D. Xu, J. Zhang, Z. Y. Sun and J. Y. Fang, *Angew. Chem., Int. Ed.*, 2008, **47**, 3540–3542; (*d*) R. G. Xie and X. G. Peng, *Angew. Chem., Int. Ed.*, 2008, **47**, 7677–7680; (*e*) M. A. Malik, P. O'Brien and M. Helliwell, *J. Mater. Chem.*, 2005, **15**, 1463–1467.

4 (*a*) F. W. Wise, *Acc. Chem. Res.*, 2000, **33**, 773–780; (*b*) B. R. Hyun, H. Y. Chen, D. A. Rey, F. W. Wise and C. A. Batt, *J. Phys. Chem. B*, 2007, **111**, 5726–5730; (*c*) W. W. Yu, J. C. Falkner, B. S. Shih and V. L. Colvin, *Chem. Mater.*, 2004, **16**, 3318–3322; (*d*) J. J. Urban, D. V. Talapin, E. V. Shevchenko and C. B. Murray, *J. Am. Chem. Soc.*, 2006, **128**, 3248–3255.

5 (*a*) P. M. Allen and M. G. Bawendi, *J. Am. Chem. Soc.*, 2008, **130**, 9240–9241; (*b*) Q. J. Guo, S. J. Kin, M. Kar, W. N. Shafarman, R. W. Birkmire, E. A. Stach, R. Agrawal and H. W. Hillhouse, *Nano Lett.*, 2008, **8**, 2982–2985; (*c*) J. Tang, S. Hinds, S. O. Kelley and E. H. Sargent, *Chem. Mater.*, 2008, **20**, 6906–6910; (*d*) R. G. Xie, M. Rutherford and X. G. Peng, *J. Am. Chem. Soc.*, 2009, **131**, 5691–5697.

6 (*a*) X. Y. Gong, H. Kan, T. Makino, T. Yamaguchi, T. Nakatskasa, M. Kumagawa, N. L. Rowell and R. Rinfret, *Cryst. Res. Technol.*, 1995, **30**, 603; (*b*) X. Marcadet, A. Rakovska, I. Rrevot, G. Glastre, B. Vinter and V. Berger, *J. Cryst. Growth*, 2001, **227–228**, 609; (*c*) V. A. Solovev, O. G. Lyublinskaya, A. N. Semenov, B. Y. Meltser, D. D. Solnyshkov, Y. V. Terentev, L. A. Prokopova, A. A. Toropov, S. V. Ivanov and P. S. Kopev, *Appl. Phys. Lett.*, 2005, **86**, 11109.

7 Z. Feit, D. Kostyk, R. J. Woods and P. Mak, *Appl. Phys. Lett.*, 1990, **57**, 2891.

8 (*a*) Y. S. Huang, L. Malikova, F. H. Pollak, H. Shen, J. Pamulapati and P. Newman, *Appl. Phys. Lett.*, 2000, **77**, 37–39; (*b*) O. J. Pitts, D. Lackner, Y. T. Cherng and S. P. Watkins, *J. Cryst. Growth*, 2008, **310**, 4858–4861; (*c*) A. Krier, M. Stone, Q. D. Zhuang, P. W. Liu and H. H. Lin, *Appl. Phys. Lett.*, 2006, **89**, 091110; (*d*) G. Ariyawansa, M. B. M. Rinzan, D. G. Esaev, S. G. Matsik, G. Hastings, A. G. U. Perera, H. C. Liu, B. N. Zvonkov and V. I. Gavrilenko, *Appl. Phys. Lett.*, 2005, **86**, 143510; (*e*) Y. Yang, W. Z. Shen, H. C. Liu, S. R. Laframboise, S. Wicaksono, S. F. Yoon and K. H. Tan, *Appl. Phys. Lett.*, 2009, **94**, 093504.

9 (*a*) S. R. Kurtz, A. A. Allerman and R. M. Biefeld, *Appl. Phys. Lett.*, 1997, **70**, 3188–3190; (*b*) V. Ciulin, S. G. Carter, M. S. Sherwin, A. Huntington and L. A. Coldren, *Phys. Rev. B: Condens. Matter Mater. Phys.*, 2004, **70**, 115312; (*c*) R. M. Biefeld, A. A. Allerman, S. R. Kurtz and J. H. Burkhart, *J. Electron. Mater.*, 1997, **26**, 1225–1230.

10 F. J. Schmitte, *Numerical Data and Functional Relationships in Science and Technology*, Landolt-Bönrstein, New Series Group III, Springer, Berlin, 1993, vol. 17 subvolume F, edited by O. Madelung, 146–152.

11 (*a*) D. Pokorná, J. Boháček, V. Vorlíček, J. Šubrt, Z. Bastl, E. A. Volnina and J. Pola, *J. Anal. Appl. Pyrolysis*, 2006, **75**, 65–68; (*b*) S. Schlecht, M. Budde and L. Kienle, *Inorg. Chem.*, 2002, **41**, 6001–6005; (*c*) C. H. An, K. B. Tang, B. Hai, G. Z. Shen, C. R. Wang and Y. T. Qian, *Inorg. Chem. Commun.*, 2003, **6**, 181; (*d*) M. V. Kovalenko, W. Heiss, E. V. Shevchenko, J. S. Lee, H. Schwinghammer, A. P. Alivisatos and D. V. Talapin, *J. Am. Chem. Soc.*, 2007, **129**, 11354–11355.

12 (*a*) J. J. Ning, Q. Q. Dai, T. Jiang, K. K. Men, D. H. Liu, N. R. Xiao, C. Y. Li, D. M. Li, B. B. Liu, B. Zou, G. T. Zou and W. W. Yu, *Langmuir*, 2009, **25**, 1818–1821; (*b*) J. J. Ning, T. Jiang, K. K. Men, Q. Q. Dai, D. M. Li, Y. J. Wei, B. B. Liu, G. Chen, B. Zou and G. T. Zou, *J. Phys. Chem. C*, 2009, **113**, 14140–14144; (*c*) K. K. Men, J. J. Ning, Q. Q. Dai, D. M. Li, B. B. Liu, W. W. Yu and B. Zou, *Colloids Surf., A*, 2010, **363**, 30–34.

13 N. Pradhan, D. Reifsnyder, R. G. Xie, J. Aldana and X. G. Peng, *J. Am. Chem. Soc.*, 2007, **129**, 9500–9509.

14 (*a*) J. Hu, L. S. Li, W. Yang, L. W. Manna and A. P. Alivisatos, *Science*, 2001, **292**, 2060; (*b*) J. Wang, M. S. Gudiksen, X. Duan, Y. Cui and C. M. Lieber, *Science*, 2001, **293**, 1455; (*c*) J. T. Hu, T. W. Odom and C. M. Lieber, *Acc. Chem. Res.*, 1999, **32**, 435; (*d*) T. Hanrath and B. A. Korgel, *J. Am. Chem. Soc.*, 2002, **124**, 1424.

15 (*a*) C. Pacholski, A. Kornowski and H. Weller, *Angew. Chem., Int. Ed.*, 2002, **41**, 1188–1191; (*b*) J. H. Yu, J. Joo, H. M. Park, S. Baik, Y. W. Kim, S. C. Kim and T. Hyeon, *J. Am. Chem. Soc.*, 2005, **127**, 5662–5670; (*c*) Z. Y. Tang, N. A. Kotov and M. Giersig, *Science*, 2002, **297**, 237–240; (*d*) X. X. Xu, J. Zhuang and X. Wang, *J. Am. Chem. Soc.*, 2008, **130**, 12527–12535; (*e*) W. Koh, A. C. Bartnik, F. W. Wise and C. B. Murray, *J. Am. Chem. Soc.*, 2010, **132**, 3909–3913.